Psychological Medicine, Page 1 of 10. © Cambridge University Press 2016
doi:10.1017/S0033291716000878

ORIGINAL ARTICLE

Connectivity of the anterior insula differentiates participants with first-episode schizophrenia spectrum disorders from controls: a machine-learning study

P. Mikolas[1,2,3,4], T. Melicher[2,3,5], A. Skoch[3,6], M. Matejka[1,2,3], A. Slovakova[1,2,3], E. Bakstein[3], T. Hajek[2,3,7]* and F. Spaniel[2,3]

[1] *Psychiatric Hospital Bohnice, Prague, Czech Republic*
[2] *3rd Faculty of Medicine, Charles University, Prague, Czech Republic*
[3] *National Institute of Mental Health, Klecany, Czech Republic*
[4] *Institute of Neuropsychiatric Care (INEP), Prague, Czech Republic*
[5] *Department of Psychiatry and Behavioral Sciences, The University of Texas Health Science Center at Houston, Houston, TX, USA*
[6] *MR Unit, Department of Diagnostic and Interventional Radiology, Institute for Clinical and Experimental Medicine, Prague, Czech Republic*
[7] *Dalhousie University, Department of Psychiatry, Halifax, Nova Scotia, Canada*

Background. Early diagnosis of schizophrenia could improve the outcomes and limit the negative effects of untreated illness. Although participants with schizophrenia show aberrant functional connectivity in brain networks, these between-group differences have a limited diagnostic utility. Novel methods of magnetic resonance imaging (MRI) analyses, such as machine learning (ML), may help bring neuroimaging from the bench to the bedside. Here, we used ML to differentiate participants with a first episode of schizophrenia-spectrum disorder (FES) from healthy controls based on resting-state functional connectivity (rsFC).

Method. We acquired resting-state functional MRI data from 63 patients with FES who were individually matched by age and sex to 63 healthy controls. We applied linear kernel support vector machines (SVM) to rsFC within the default mode network, the salience network and the central executive network.

Results. The SVM applied to the rsFC within the salience network distinguished the FES from the control participants with an accuracy of 73.0% ($p = 0.001$), specificity of 71.4% and sensitivity of 74.6%. The classification accuracy was not significantly affected by medication dose, or by the presence of psychotic symptoms. The functional connectivity within the default mode or the central executive networks did not yield classification accuracies above chance level.

Conclusions. Seed-based functional connectivity maps can be utilized for diagnostic classification, even early in the course of schizophrenia. The classification was probably based on trait rather than state markers, as symptoms or medications were not significantly associated with classification accuracy. Our results support the role of the anterior insula/salience network in the pathophysiology of FES.

Received 9 June 2015; Revised 4 April 2016; Accepted 5 April 2016

Key words: First-episode schizophrenia spectrum, functional connectivity, functional magnetic resonance imaging, machine learning, salience network.

Introduction

Schizophrenia is often a chronic, life-long condition with an early onset (Rabinowitz *et al.* 2007; Andreasen *et al.* 2011). It accounts for 1.1% of the total disability-adjusted life years (DALYs) and 2.8% of years lived with disability (Levav & Rutz, 2002) and is the eighth leading cause of DALYs worldwide in the 15–44 years age group. Delayed diagnosis may result in brain structural/functional alterations (Penttilä *et al.* 2010; Guo *et al.* 2013, 2015), which complicate the treatment and may result in poor cognitive and social functioning (Malla *et al.* 2011). Therefore, the study of participants during their first episode of schizophrenia spectrum disorders (FES) is of high relevance, as it could improve early diagnosis. By limiting the effects of illness burden and medication exposure (Lieberman *et al.* 2001; Smieskova *et al.* 2009; Ho *et al.* 2011), this approach could also help identify biological signatures of the illness.

Brain imaging provides an interesting tool for the study of psychiatric disorders. Yet, the diagnostic

* Address for correspondence: T. Hajek, M.D., Ph.D., Dalhousie University, Department of Psychiatry, QEII HSC, A.J. Lane Bldg, Room 3093, 5909 Veteran's Memorial Lane, Halifax, NS B3H 2E2, Canada.
(Email: tomas.hajek@dal.ca)

promise of neuroimaging in psychiatry has not yet been fully realized. The main reasons for this pertain to clinical heterogeneity and low sensitivity/specificity of brain imaging findings. The former issue can be addressed by studying more homogeneous patient populations, such as participants at the early stages of the illness. The later problem can be resolved by novel methods of magnetic resonance imaging (MRI) data analysis, such as machine learning (ML). Unlike conventional univariate methods, which yield significant results on a group level, multivariate ML classifiers are sensitive enough to accurately classify individual subjects (Haller *et al.* 2014; Sundermann *et al.* 2014, Koutsouleris *et al.* 2015). Moreover, multivariate patterns of brain changes, such as those detected by ML, may be more characteristic of psychiatric disorders (Davatzikos *et al.* 2005). Thus, ML may help bring neuroimaging from the bench to the bedside (Hajek *et al.* 2015).

Schizophrenia has been associated with aberrant functional connectivity (FC) within and between the default mode network (DMN), the central executive network (CEN) and the salience network (SN) (Palaniyappan *et al.* 2013; Manoliu *et al.* 2014; Nekovarova *et al.* 2014; Spaniel *et al.* 2016). Thus we investigated whether patterns of resting-state FC (rsFC), within these networks, would allow us to differentiate healthy controls from participants at the early stages of schizophrenia.

ML applied to resting-state functional MRI (rsfMRI) was successfully used to classify patients with an established illness (Kambeitz *et al.* 2015). However, to the best of our knowledge, this is the first study to use rsFC to differentiate participants with a FES from healthy controls. In addition, we compared the results obtained by ML with those derived from traditional between-group FC analyses.

Method

Study design

We recruited participants through the Early-Stage Schizophrenia Outcome study (ESO), a prospective trial of FES subjects, conducted in Prague and the Central Bohemia areas (Melicher *et al.* 2015). The study was carried out in accordance with the latest version of the Declaration of Helsinki. A written informed consent was obtained from all of the subjects and the local ethics committee approved the protocol.

Patients with FES

We recruited patients hospitalized at the Bohnice Psychiatric Hospital, Prague. The inclusion criteria were: (1) the diagnosis of schizophrenia or the diagnosis of an acute polymorphic psychotic disorder, as made by a psychiatrist, according to the International Classification of Diseases-10 criteria; (2) the first episode of psychotic illness; (3) the duration of untreated psychosis $\leqslant$24 months. Any patients with psychotic mood disorders (including schizo-affective disorder, bipolar disorder, and unipolar depression with psychotic symptoms) were excluded from the study. All of the patients were treated with antipsychotic drugs at the time of the MRI scanning. We rated the symptom severity using the Positive and Negative Syndrome Scale (PANSS) (Kay *et al.* 1987).

The MRI scanning was performed during the first hospitalization, as soon as the patients were able to understand the purpose of the study and undergo the fMRI protocol. As participants were typically hospitalized shortly after developing symptoms, some of them did not meet the duration criteria for schizophrenia at the time of scanning. These patients received the working diagnosis of acute polymorphic psychotic disorder.

Healthy controls

The healthy control subjects were recruited via an advertisement from a similar sociodemographic background and were matched to FES participants by age and sex on an individual basis. The main exclusion criteria for the control subjects were a personal lifetime history of any psychiatric disorder, or any substance abuse, established by the Mini International Neuropsychiatric Interview (M.I.N.I.) (Lecrubier *et al.* 1997). We also excluded any family history of a psychiatric illness in first- or second-degree relatives (see Table 1 for details).

Further exclusion criteria, for both the patients and the healthy controls, included current neurological disorders, a lifetime history of seizures, or a head injury with altered consciousness, an intracranial hemorrhage, history of mental retardation, substance dependence, and any contraindications for MRI scanning.

fMRI data acquisition

The data were acquired by a 3 T Siemens Trio MRI scanner (Germany) equipped with a standard head coil. For the fMRI data pre-processing, the subjects were scanned using a structural T1-weighted three-dimensional MPRAGE sequence [repetition time (TR) 2300 ms, echo time (TE) 4.63 ms, bandwidth 130 Hz/pixel, field of view (FOV) 256 × 256 mm, matrix 256 × 256, 160–224 contiguous sagittal slices, a voxel size of $1 \times 1 \times 1$ mm^3, GRAPPA, and Acceleration Factor 2]. Functional images sensitive to the blood oxygen level-dependent (BOLD) contrast were measured with a gradient echo echo-planar sequence (GRE-EPI, TR = 2000 ms, TE = 30 ms, flip angle 90°, bandwidth 2232 Hz/pixel, without parallel acceleration, FOV = 192 mm × 144 mm, matrix size 64 × 48, a voxel size of $3 \times 3 \times 3$

Table 1. *Demographic and clinical characteristics of the participants*

	Controls ($n = 63$)	Patients ($n = 63$)	Statistics
Sex, *n* female (% female)	24 (38)	24 (38)	$\chi^2 = 0$, df = 1, $p = 1$
Mean age, years (S.D.)	28.1 (6.3)	28.8 (6.2)	$t = 0.61$, df = 124, $p = 0.54$
Diagnosis, *n* (%)			
Schizophrenia	N.A.	37 (58.7)	
Acute polymorphic psychotic disorder	N.A.	26 (41.3)[a]	
Duration of illness, months			
Mean	N.A.	2[b]	N.A.
Median (interquartile range)	N.A.	2 (0–24)[b]	N.A.
Median antipsychotic dose at the time of scanning, mg chlorpromazine equivalents (interquartile range)	N.A.	375 (289.5)	N.A.
Mean PANSS score (S.D.)			
Positive	N.A.	16.9 (6.7)	N.A.
Negative	N.A.	16.9 (6.4)	N.A.
General	N.A.	36.3 (9.2)	N.A.
Total	N.A.	70.1 (17.7)	N.A.

df, Degrees of freedom; S.D., standard deviation; N.A., not applicable; PANSS, Positive and Negative Syndrome Scale.

[a] A total of 13 patients received the working diagnosis of acute polymorphic psychotic disorder, because they did not meet the duration criteria for schizophrenia at the time of scanning.

[b] Data missing for six patients.

mm^3, each volume with 35 axial slices without an inter-slice gap, and a total of 400 volumes).

fMRI data processing

Functional/structural data were pre-processed and analysed using tools implemented in the MATLAB 7.14 (R2012a) software. Slice-timing, realignment, regression of nuisance covariates (white matter and cerebrospinal fluid signal, voxel specific head motion, mean signal), spatial normalization and smoothing of the functional images, as well as spatial normalization of the structural T1 images, were performed by an SPM8-Data Processing Based Toolbox Assistant for the Resting-fMRI (DPARSF) (Chao-Gan & Yu-Feng, 2010), and the Resting-State fMRI Data Analysis Toolkit (REST) (Song *et al.* 2011). The images were smoothed with an 8 × 8 × 8 Gaussian kernel. We applied temporal filtering over the frequency band of 0.008–0.09 Hz.

FC analysis

rsFC for all of the subjects was calculated between pre-selected regions of interest (ROIs) and the voxels in the rest of the brain (seed-based connectivity), using pre-processing pipelines which are well established and often used in the field (i.e. Craddock *et al.* 2009; Alonso-Solís *et al.* 2012; Venkataraman *et al.* 2012). We selected three ROIs, which correspond to the three networks of interest, i.e. posterior cingulate gyrus for the DMN, dorsolateral prefrontal cortex (DLPFC), as represented by the middle frontal gyrus for the CEN and anterior insula for the SN. The posterior cingulate gyrus and the DLPFC were selected from the Automated Anatomical Labeling (AAL) atlas (Tzourio-Mazoyer *et al.* 2002). This atlas does not provide parcellation of insula, which we obtained from Freesurfer (sulcus circular insulae) (Fischl *et al.* 2004; Sridharan *et al.* 2008; Destrieux *et al.* 2010; Menon & Uddin, 2010; Palaniyappan *et al.* 2013). As patients with established schizophrenia as well as those with FES show reduced asymmetry of rsFC, we used ROIs from both sides as seeds in each model (Damoiseaux *et al.* 2006; Swanson *et al.* 2011; Cabral *et al.* 2014; Guo *et al.* 2014). Thus, for each subject, we calculated three connectivity maps, including connectivity between: (1) bilateral anterior insula; (2) bilateral posterior cingulate; (3) bilateral middle frontal gyrus and the rest of the brain. Correlation coefficients were transformed into *Z*-scores by Fisher's transformation. These first-level, individual subject connectivity maps were subjected to ML; see the support vector machines (SVM) classification paragraph below.

The second-level FC analysis was performed by the SPM8-Data Processing Based Toolbox Assistant. The differences in the seed-based FC between the patients and the controls were tested using a two-sample *t* test. The results were family-wise error corrected with a significance threshold of $p < 0.05$ on a cluster level. Only clusters exceeding 20 voxels were considered significant. In order to compare the uncorrected differences in the seed-based FC with the weight distribution obtained by the SVM, we performed a *t* test on an uncorrected level, with a cluster level of $p = 0.001$.

SVM classification

We applied a linear kernel support-vector classifier (SVM) implemented in the PRONTO toolbox v 1.1 (Schrouff *et al.* 2013) to the individual subject FC maps. We estimated three separate SVM classification models (one for each of the three ROIs corresponding to the three pre-selected resting-state networks). In

order to remove zero voxels, all normalized brains were extracted using a BET tool implemented in the FSL package (Smith *et al.* 2004) and multiplied with each other in order to generate a common mask. The ML analyses were restricted to gray matter, by using a normalized gray matter mask provided by Dr Wager's laboratory (http://wagerlab.colorado.edu/wiki/doku.php/help/core/brain_masks). Each FC map comprised 52941 voxels (features).

This study utilized a linear kernel SVM, which is less prone to overfitting than non-linear SVMs. Linear kernel SVMs have a single parameter, C, that controls the trade-off between having zero training errors and allowing misclassifications. Similar to other studies, we used the default parameter $C = 1$ (Mourao-Miranda *et al.* 2012; Rocha-Rego *et al.* 2014; Hajek *et al.* 2015). It has been shown previously by LaConte *et al.* (2005) that the SVM performance for whole-brain classification does not change for a large range of C values and only degrades with very small C values. Thus, modifying the C threshold was suggested only when the dimensionality of the data is smaller than the number of examples (e.g. classification based on small ROIs), which was not the case in our study. Others have suggested that using a sample-dependent optimization of the parameter C may improve the performance of the model (Franke *et al.* 2010; Nieuwenhuis *et al.* 2012). However, the aim of this study was not to optimise the SVM methods. Our goal was to reduce the methodological heterogeneity and use a simple, 'out of the box' approach, which could be applicable in clinical setting (Mourao-Miranda *et al.* 2012).

We performed a leave-one-subject-per-group-out cross-validation. This means, that on each run, one subject from each group was assigned to a testing set and the remaining subjects were assigned to a learning set. The classification was then performed on the two subjects in the test set. This was repeated until all of the subjects had been tested. During the cross-validation procedure, all of the patients were matched with the healthy controls according to age and sex. The classification accuracy was expressed as a total performance on all runs. The statistical significance of the obtained classification accuracy was tested on 1000 randomly permuted datasets, with a random assignment of the group class to the input image. A resulting null-hypothesis distribution was used to calculate the p value of the accuracies, i.e. the proportion of the permutations that yielded a greater accuracy than the accuracy found for the classification models.

Analysis of the effects of medication and symptoms

We attempted to clarify the contribution of medication and symptoms in several ways: (1) we compared symptoms and medication dose between correctly and incorrectly classified subjects using an independent-sample t test; (2) we used a linear regression to assess the association between classification accuracy (value of the SVM decision function) and medication dose [expressed as chlorpromazine (CPZ) equivalents] or symptoms; (3) we modeled the effects of covariates on FC. Of note, in ML, removal of confounding covariates can violate the basic train/test assumption by introducing the information about the whole dataset before introducing labels. Therefore covarying for medication dose or symptoms would not be optimal. To counter this problem, we thus used another ML approach – Gaussian process regression (GPR). Using the complex GPR model makes few assumptions about the shape of the possible relationship and is thus more powerful than linear models (Rasmussen & Williams, 2006; Schrouff *et al.* 2013). Using linear model in this case could easily lead to underfitting in the case of a non-linear relationship. Therefore, by harvesting as much of the confounding relationship as possible, the GPR ensures that we exhaustively investigated and quantified the contribution of potential confounding factors to our findings. Specifically, we performed a GPR in order to estimate the CPZ dose, or the total PANSS and three subscales (positive, negative, general), on the day of scanning from the FC maps (Rasmussen & Williams, 2006). We only applied these analyses to networks, which differentiated FES from controls above chance level. All analyses were performed by the PRoNTo Toolbox v.1.1 (Schrouff *et al.* 2013).

Ethical standards

All procedures contributing to this work comply with the ethical standards of the relevant national and institutional committees on human experimentation and with the Helsinki Declaration of 1975, as revised in 2008.

Results

Demographic data

We recruited 63 FES participants who were individually matched by age and sex to 63 healthy controls, without a personal or a family history of psychiatric disorder; see Table 1 for a description of the samples.

Support vector classification of FES and control participants

ML applied to rsFC within the SN differentiated FES from the control participants with specificity of 71.4% ($p = 0.001$), sensitivity of 74.6% ($p = 0.001$), and balanced accuracy of 73.0% ($p = 0.001$, area under the receiver

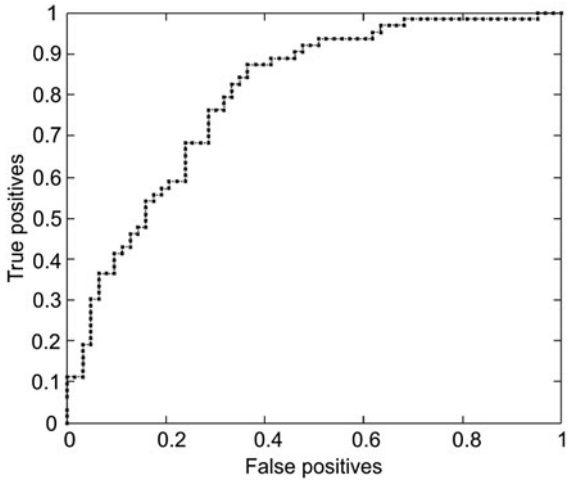

Fig. 1. The receiver operating characteristic (ROC) curve for the classification model was based on functional connectivity maps of the anterior insula. The ROC curve shows the sensitivity *v.* specificity trade-off and the area under the curve (0.80). True positives = sensitivity; false positives = 1 − specificity.

operating characteristic curve = 0.80, Fig. 1). In other words, among the 63 FES subjects, 16 individuals were mislabeled as being controls, whereas 18 out of 63 controls were incorrectly classified as FES. The regions which most contributed to the discrimination of the two groups contained the anterior and posterior cingulate, precuneus, ventro- and dorsolateral prefrontal cortex, angular and supramarginal gyri, temporo-occipital regions, lingular gyrus, and thalamus. The FC within the other networks, i.e. the DMN and CEN, did not yield classifications above chance level (see Table 2).

FC analysis – between-group comparisons

There were no significant differences in rsFC between the FES and the control participants on a corrected level for either of the seed regions, i.e. the posterior cingulate cortex, dorsolateral prefrontal cortex and anterior insula. We further tested differences in rsFC of the anterior insula on an uncorrected level. The uncorrected comparisons yielded between-group connectivity differences in the bilateral angular and supramarginal gyri. These regions closely overlapped with the maximum weight vectors obtained from the ML classification model based on SN connectivity (Fig. 2)

Effects of medication and psychotic symptoms

The correctly classified patients did not differ from the misclassified ones in PANSS scores [$t = 0.08$, degrees of freedom (df) = 61, $p = 0.9$] or medication dose ($t = -1.66$, df = 60, $p = 0.1$). There was no association between classification accuracy and CPZ equivalents ($r = -0.21$, $p = 0.11$) or symptoms ($r = -0.07$, $p = 0.58$). Lastly, ML (GPR) was unable to estimate the CPZ dose ($r = 0.22$, $p = 0.09$) or the current symptoms as measured by the PANSS total scores or subscales (PANSS-total, $r = -0.03$, $p = 0.81$; PANSS-pos, $r = -0.09$, $p = 0.472$; PANSS-neg, $r = 0.17$, $p = 0.184$; PANSS-gen, $r = -0.03$, $p = 0.81$) from the rsFC within the SN.

Discussion

In this study, whole-brain rsFC maps of the anterior insula/SN differentiated FES participants from controls with an above-chance accuracy of 73%, specificity of 71.4% and sensitivity of 74.6%. The classification was not significantly affected by medication dose, or by the presence of psychotic symptoms, and thus was probably based on trait rather than state markers.

Our findings provide a proof of concept that rsfMRI can be successfully used to differentiate participants with FES from healthy controls. rsfMRI is particularly suitable for diagnostic classification (Craddock *et al.* 2009; Haller *et al.* 2014). Compared with task-based fMRI paradigms, the resting-state approach reduces the amount of bias introduced by task non-adherence. This is an important advantage in participants with FES, who tend to have distorted perception and impaired cognitive functioning. Also the rsFC seed regions can be selected *a priori* from pre-defined atlases, which makes this approach transferable among independent groups of subjects. Although it is difficult to directly compare the results due to the methodological differences, the classification performance obtained by using rsFC in this study was comparable with the sensitivity and specificity obtained from structural MRI and rsfMRI in established schizophrenia patients and FES as reported in a recent meta-analysis by Kambeitz *et al.* (2015) (sensitivity 76% and specificity 79% for structural MRI, sensitivity 84% and specificity 77% for rsfMRI). Studies that focused on FES exclusively have reported accuracies ranging from 65.8 to 94% for structural MRI (Kasparek *et al.* 2011; Takayanagi *et al.* 2011; Borgwardt & Fusar-Poli, 2012; Pettersson-Yeo *et al.* 2013; Zanetti *et al.* 2013).

The anterior insula is a crucial component of the SN. The disruption of anterior insula and SN connectivity has been well documented in schizophrenia (White *et al.* 2010; Moran *et al.* 2013; Palaniyappan *et al.* 2013; Manoliu *et al.* 2014; Iwabuchi *et al.* 2015). Additionally, a gray matter reduction within the insula has been consistently and robustly reported in meta-analyses of morphometric MRI studies in schizophrenia (Glahn *et al.* 2008; Ellison-Wright & Bullmore, 2010; Bora *et al.* 2011; Palaniyappan *et al.* 2013). However, the specificity of these changes to schizophrenia is unclear. Recent

Table 2. *Results of the support vector machine classification of patients with a first-episode schizophrenia spectrum disorder and healthy controls from the whole-brain seed-based functional connectivity maps*[a]

ROI	Sensitivity	*p*	Specificity	*p*	Balanced accuracy	*p*, Balanced	AUC[b]
Posterior cingulate cortex	54.0	0.292	57.1	0.155	55.6	0.176	0.55
Dorsolateral prefrontal cortex	57.1	0.133	58.7	0.09	57.9	0.072	0.62
Anterior insula	74.6	0.001	71.4	0.001	73.0	0.001	0.80

ROI, Region of interest; AUC, area under receiver operating characteristic curve.
[a] *p* Values were calculated from permutation testing with 1000 permutations.
[b] See Fig. 1 for details.

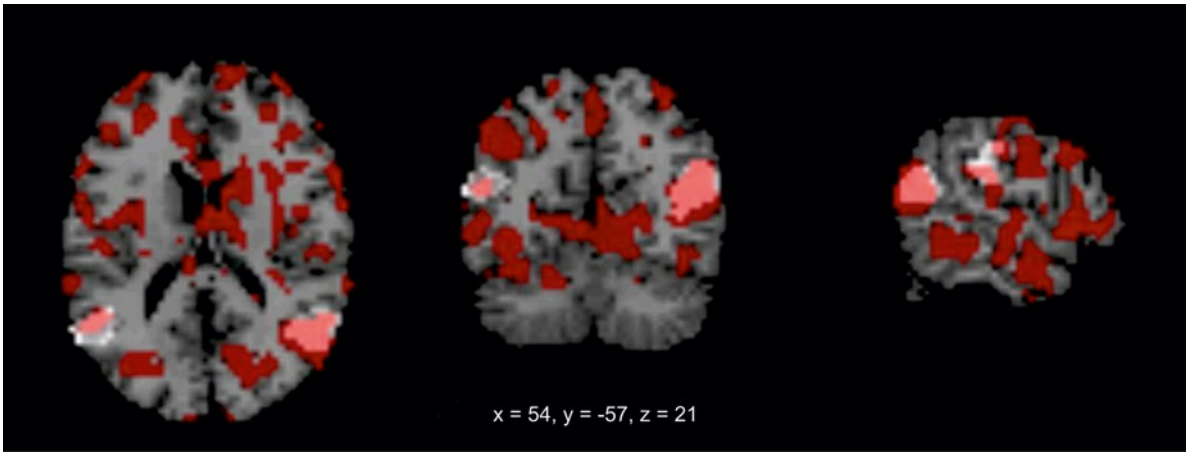

Fig. 2. Comparison of the regions contributing to the classification based on salience network connectivity obtained by machine learning (red) with differences between the patients with first episode of schizophrenia-spectrum disorder and controls in salience network connectivity (white). Differences in functional connectivity between the patients and the controls were obtained as *F*-contrast ($p = 0.001$, cluster-level uncorrected).

findings suggest that a general mapping exists between a broad range of psychiatric symptoms and the integrity of an anterior insula-based network across a wide variety of neuropsychiatric illnesses (Goodkind *et al.* 2015).

Although the DMN and CEN exhibit functional abnormalities in schizophrenia (Ren *et al.* 2013; Spaniel *et al.* 2016), we did not achieve above-chance classifications when we focused on connectivity within these networks. We also did not identify any significant between-group FC differences in these networks. One explanation may lie in the dynamics of structural brain changes during the course of an illness. Some studies suggest that abnormalities of insular cortex in psychotic disorders may reflect pre-existing vulnerability. Later in the course of illness, the changes secondary to the illness burden may lead to the extension of these alterations to other neighboring structures (Takahashi *et al.* 2009; Chan *et al.* 2011). However, other studies do not support this view of dynamic pattern changes in brain morphology (Vita *et al.* 2012).

Another explanation is that previous findings reflect clinical heterogeneity *vis-à-vis* the clinical course. Recent studies have demonstrated that classification accuracies are higher in participants with chronic course of illness, and lower in those with an episodic illness. Perhaps the presence of patients who will go on to develop an episodic illness could have decreased the prediction accuracies for some of the networks (Mourao-Miranda *et al.* 2012; Gould *et al.* 2014).

It is of note that even the between-group differences in the anterior insula connectivity did not reach statistical significance. However, on an uncorrected level, the localization of group differences overlapped with the regions with a maximum contribution to the classification using ML. Due to the multivariate nature, which obviates the need to control for multiple comparisons, ML appears to be more sensitive than conventional mass univariate approaches.

This study has the following limitations. A common problem in ML is overfitting (Whelan & Garavan, 2014). We used a linear-kernel SVM classifier, which

was shown to have a low likelihood of overfitting in fMRI paradigms (LaConte *et al.* 2005; Mourao-Miranda *et al.* 2012). In addition, two out of three of our models failed to produce significant results, which makes overfitting unlikely.

Unlike the healthy controls, all of the patients were on antipsychotic medication and experienced mild psychotic symptoms at the time of scanning. However, there was no significant association between symptoms or medication dose and classification accuracy. Likewise, ML was unable to estimate symptom levels or medication dose from rsFC data. Last but not least, there were no significant differences between the correctly and incorrectly classified subjects in symptom levels or medication dose. Thus, it is unlikely that medication or psychotic symptoms markedly contributed to the classification. There are a limited number of studies focusing on correlations of clinical symptom severity and/or medication dose with rsFC in FES. The results differ depending on the regions of interest. Some studies have found positive as well as negative correlations of striatal connectivity with symptom severity that was resolved with treatment (Sarpal *et al.* 2015). However, another study reported no correlations between symptom severity and rsFC of the DMN (Alonso-Solís *et al.* 2012).

We were primarily interested in subjects at the early stages of illness, as this is one of the few ways how to limit the effects of previous psychotic episodes and how to minimize exposure to medications or comorbid conditions. This approach minimizes the effects of confounding variables, which could alter classification accuracy. Consequently, as many of the participants were hospitalized shortly after developing symptoms, some of them did not meet the duration criteria for schizophrenia at the time of scanning. These patients received the working diagnosis of acute polymorphic psychotic disorder.

As this is an emerging field, there is no standardization of the methods of data pre-processing and analyses for the ML studies. We do not know exactly the influence of individual processing steps or selection of ROI on the outcomes. At the same time, the SVMs are among the most used ML classifiers in psychiatric neuroimaging (Sundermann *et al.* 2014).

Consequently, we used SVM with the default parameters in order to decrease the methodological heterogeneity and to ensure comparability with other studies. This way, we showed that even a simple 'out of the box', easily applicable classifier with linear (hyperplane) decision boundary could correctly distinguish between patients and controls. For the same reason, we used standard atlases to select the ROIs, which are representative of the individual networks. In future studies, it would be interesting to test other classifiers, such as random forest or discriminant analyses, or to focus on different ROIs.

To conclude, this study provides a proof of concept that ML of seed-based rsFC maps can be utilized for the diagnostic classification of participants early in the course of schizophrenia. We were able to discriminate patients with FES from healthy controls with an accuracy of 73%. Furthermore, our results emphasize the role of rsFC within the SN in the pathophysiology of FES. Future studies should attempt to use this approach in unaffected individuals at a genetic risk of schizophrenia, should aim to test the specificity of the results to schizophrenia and might benefit from novel classification algorithms.

Acknowledgements

The study was supported by: the Ministry of Health, Czech Republic (F.S., grant number 16-32696A); the Ministry of Health, Czech Republic – Conceptual Development of Research Organization 00023001 [Institut klinické a experimentální medicíny (IKEM), Prague, Czech Republic] – Institutional support; and Charles University, Prague (grant number 260168/SVV/2015).

The funding source had no role in the study design, the collection analysis, the interpretation of data, the writing of the paper, or in the decision for publication.

F.S., T.H. and P.M. designed the study; F.S., P.M., A. Sl. and M.M. participated in the patient recruitment; they also performed clinical examinations and scales. T.M. analysed the subject cohort demographics; P.M. and A.Sk. performed the fMRI pre-processing; P.M., E.B. and T.H. performed the fMRI data analyses and statistics; P.M., F.S. and T.H. wrote the article, which all of the authors reviewed and approved for publication.

Declaration of Interest

None.

References

Alonso-Solís A, Corripio I, de Castro-Manglano P, Duran-Sindreu S, Garcia-Garcia M, Proal E, Nuñez-Marín F, Soutullo C, Alvarez E, Gómez-Ansón B, Kelly C, Castellanos FX (2012). Altered default network resting state functional connectivity in patients with a first episode of psychosis. *Schizophrenia Research* **139**, 13–18.

Andreasen NC, Nopoulos P, Magnotta V, Pierson R, Ziebell S, Ho B-C (2011). Progressive brain change in schizophrenia: a prospective longitudinal study of first-episode schizophrenia. *Biological Psychiatry* **70**, 672–679.

Bora E, Fornito A, Radua J, Walterfang M, Seal M, Wood SJ, Yücel M, Velakoulis D, Pantelis C (2011).

Neuroanatomical abnormalities in schizophrenia: a multimodal voxelwise meta-analysis and meta-regression analysis. *Schizophrenia Research* **127**, 46–57.

Borgwardt S, Fusar-Poli P (2012). Third-generation neuroimaging in early schizophrenia: translating research evidence into clinical utility. *British Journal of Psychiatry: The Journal of Mental Science* **200**, 270–272.

Cabral J, Kringelbach ML, Deco G (2014). Exploring the network dynamics underlying brain activity during rest. *Progress in Neurobiology* **114**, 102–131.

Chan RCK, Di X, McAlonan GM, Gong Q (2011). Brain anatomical abnormalities in high-risk individuals, first-episode, and chronic schizophrenia: an activation likelihood estimation meta-analysis of illness progression. *Schizophrenia Bulletin* **37**, 177–188.

Chao-Gan Y, Yu-Feng Z (2010). DPARSF: A MATLAB toolbox for 'pipeline' data analysis of resting-state fMRI. *Frontiers in Systems Neuroscience* **4**, 13.

Craddock RC, Holtzheimer PE, Hu XP, Mayberg HS (2009). Disease state prediction from resting state functional connectivity. *Magnetic Resonance in Medicine: Official Journal of the Society of Magnetic Resonance in Medicine/Society of Magnetic Resonance in Medicine* **62**, 1619–1628.

Damoiseaux JS, Rombouts SARB, Barkhof F, Scheltens P, Stam CJ, Smith SM, Beckmann CF (2006). Consistent resting-state networks across healthy subjects. *Proceedings of the National Academy of Sciences* **103**, 13848–13853.

Davatzikos C, Shen D, Gur RC, Wu X, Liu D, Fan Y, Hughett P, Turetsky BI, Gur RE (2005). Whole-brain morphometric study of schizophrenia revealing a spatially complex set of focal abnormalities. *Archives of General Psychiatry* **62**, 1218–1227.

Destrieux C, Fischl B, Dale A, Halgren E (2010). Automatic parcellation of human cortical gyri and sulci using standard anatomical nomenclature. *NeuroImage* **53**, 1–15.

Ellison-Wright I, Bullmore E (2010). Anatomy of bipolar disorder and schizophrenia: a meta-analysis. *Schizophrenia Research* **117**, 1–12.

Fischl B, Salat DH, van der Kouwe AJW, Makris N, Ségonne F, Quinn BT, Dale AM (2004). Sequence-independent segmentation of magnetic resonance images. *NeuroImage* **23** (Suppl. 1), S69–S84.

Franke K, Ziegler G, Klöppel S, Gaser C (2010). Estimating the age of healthy subjects from T1-weighted MRI scans using kernel methods: exploring the influence of various parameters. *NeuroImage* **50**, 883–892.

Glahn DC, Laird AR, Ellison-Wright I, Thelen SM, Robinson JL, Lancaster JL, Bullmore E, Fox PT (2008). Meta-analysis of gray matter anomalies in schizophrenia: application of anatomic likelihood estimation and network analysis. *Biological Psychiatry* **64**, 774–781.

Goodkind M, Eickhoff SB, Oathes DJ, Jiang Y, Chang A, Jones-Hagata LB, Ortega BN, Zaiko YV, Roach EL, Korgaonkar MS, Grieve SM, Galatzer-Levy I, Fox PT, Etkin A (2015). Identification of a common neurobiological substrate for mental illness. *JAMA Psychiatry* **72**, 305–315.

Gould IC, Shepherd AM, Laurens KR, Cairns MJ, Carr VJ, Green MJ (2014). Multivariate neuroanatomical classification of cognitive subtypes in schizophrenia: a support vector machine learning approach. *NeuroImage Clinical* **6**, 229–236.

Guo W, Liu F, Xiao C, Yu M, Zhang Z, Liu J, Zhang J, Zhao J (2015). Increased causal connectivity related to anatomical alterations as potential endophenotypes for schizophrenia. *Medicine* **94**, e1493.

Guo W, Xiao C, Liu G, Wooderson SC, Zhang Z, Zhang J, Yu L, Liu J (2014). Decreased resting-state interhemispheric coordination in first-episode, drug-naive paranoid schizophrenia. *Progress in Neuro-Psychopharmacology and Biological Psychiatry* **48**, 14–19.

Guo X, Li J, Wei Q, Fan X, Kennedy DN, Shen Y, Chen H, Zhao J (2013). Duration of untreated psychosis is associated with temporal and occipitotemporal gray matter volume decrease in treatment naïve schizophrenia. *PLOS ONE* **8**, e83679.

Hajek T, Cooke C, Kopecek M, Novak T, Hoschl C, Alda M (2015). Using structural MRI to identify individuals at genetic risk for bipolar disorders: a 2-cohort, machine learning study. *Journal of Psychiatry and Neuroscience: JPN* **40**, 316–324.

Haller S, Lovblad K-O, Giannakopoulos P, Van De Ville D (2014). Multivariate pattern recognition for diagnosis and prognosis in clinical neuroimaging: state of the art, current challenges and future trends. *Brain Topography* **27**, 329–337.

Ho B-C, Andreasen NC, Ziebell S, Pierson R, Magnotta V (2011). Long-term antipsychotic treatment and brain volumes: a longitudinal study of first-episode schizophrenia. *Archives of General Psychiatry* **68**, 128–137.

Iwabuchi SJ, Liddle PF, Palaniyappan L (2015). Structural connectivity of the salience-executive loop in schizophrenia. *European Archives of Psychiatry and Clinical Neuroscience* **265**, 163–166.

Kambeitz J, Kambeitz-Ilankovic L, Leucht S, Wood S, Davatzikos C, Malchow B, Falkai P, Koutsouleris N (2015). Detecting neuroimaging biomarkers for schizophrenia: a meta-analysis of multivariate pattern recognition studies. *Neuropsychopharmacology: Official Publication of the American College of Neuropsychopharmacology* **40**, 1742–1751.

Kasparek T, Thomaz CE, Sato JR, Schwarz D, Janousova E, Marecek R, Prikryl R, Vanicek J, Fujita A, Ceskova E (2011). Maximum-uncertainty linear discrimination analysis of first-episode schizophrenia subjects. *Psychiatry Research* **191**, 174–181.

Kay SR, Fiszbein A, Opler LA (1987). The Positive and Negative Syndrome Scale (PANSS) for schizophrenia. *Schizophrenia Bulletin* **13**, 261–276.

Koutsouleris N, Meisenzahl EM, Borgwardt S, Riecher-Rössler A, Frodl T, Kambeitz J, Köhler Y, Falkai P, Möller H-J, Reiser M, Davatzikos C (2015). Individualized differential diagnosis of schizophrenia and mood disorders using neuroanatomical biomarkers. *Brain: A Journal of Neurology* **138**, 2059–2073.

LaConte S, Strother S, Cherkassky V, Anderson J, Hu X (2005). Support vector machines for temporal classification of block design fMRI data. *NeuroImage* **26**, 317–329.

Lecrubier Y, Sheehan DV, Weiller E, Amorim P, Bonora I, Harnett Sheehan K, Janavs J, Dunbar GC (1997). The Mini International Neuropsychiatric Interview (MINI). A short

diagnostic structured interview: reliability and validity according to the CIDI. *European Psychiatry* **12**, 224–231.

Levav I, Rutz W (2002). The WHO World Health Report 2001 new understanding – new hope. *Israel Journal of Psychiatry and Related Sciences* **39**, 50–56.

Lieberman J, Chakos M, Wu H, Alvir J, Hoffman E, Robinson D, Bilder R (2001). Longitudinal study of brain morphology in first episode schizophrenia. *Biological Psychiatry* **49**, 487–499.

Malla AK, Bodnar M, Joober R, Lepage M (2011). Duration of untreated psychosis is associated with orbital–frontal grey matter volume reductions in first episode psychosis. *Schizophrenia Research* **125**, 13–20.

Manoliu A, Riedl V, Zherdin A, Muhlau M, Schwerthoffer D, Scherr M, Peters H, Zimmer C, Forstl H, Bauml J, Wohlschlager AM, Sorg C (2014). Aberrant dependence of default mode/central executive network interactions on anterior insular salience network activity in schizophrenia. *Schizophrenia Bulletin* **40**, 428–437.

Melicher T, Horacek J, Hlinka J, Spaniel F, Tintera J, Ibrahim I, Mikolas P, Novak T, Mohr P, Hoschl C (2015). White matter changes in first episode psychosis and their relation to the size of sample studied: a DTI study. *Schizophrenia Research* **162**, 22–28.

Menon V, Uddin LQ (2010). Saliency, switching, attention and control: a network model of insula function. *Brain Structure and Function* **214**, 655–667.

Moran LV, Tagamets MA, Sampath H, O'Donnell A, Stein EA, Kochunov P, Hong LE (2013). Disruption of anterior insula modulation of large-scale brain networks in schizophrenia. *Biological Psychiatry* **74**, 467–474.

Mourao-Miranda J, Reinders AATS, Rocha-Rego V, Lappin J, Rondina J, Morgan C, Morgan KD, Fearon P, Jones PB, Doody GA, Murray RM, Kapur S, Dazzan P (2012). Individualized prediction of illness course at the first psychotic episode: a support vector machine MRI study. *Psychological Medicine* **42**, 1037–1047.

Nekovarova T, Fajnerova I, Horacek J, Spaniel F (2014). Bridging disparate symptoms of schizophrenia: a triple network dysfunction theory. *Frontiers in Behavioral Neuroscience* **8**, 171.

Nieuwenhuis M, van Haren NEM, Hulshoff Pol HE, Cahn W, Kahn RS, Schnack HG (2012). Classification of schizophrenia patients and healthy controls from structural MRI scans in two large independent samples. *NeuroImage* **61**, 606–612.

Palaniyappan L, Simmonite M, White TP, Liddle EB, Liddle PF (2013). Neural primacy of the salience processing system in schizophrenia. *Neuron* **79**, 814–828.

Penttilä M, Jääskeläinen E, Haapea M, Tanskanen P, Veijola J, Ridler K, Murray GK, Barnes A, Jones PB, Isohanni M, Koponen H, Miettunen J (2010). Association between duration of untreated psychosis and brain morphology in schizophrenia within the Northern Finland 1966 Birth Cohort. *Schizophrenia Research* **123**, 145–152.

Pettersson-Yeo W, Benetti S, Marquand AF, Dell'Acqua F, Williams SCR, Allen P, Prata D, McGuire P, Mechelli A (2013). Using genetic, cognitive and multi-modal neuroimaging data to identify ultra-high-risk and first-episode psychosis at the individual level. *Psychological Medicine* **43**, 2547–2562.

Rabinowitz J, Levine SZ, Haim R, Häfner H (2007). The course of schizophrenia: progressive deterioration, amelioration or both? *Schizophrenia Research* **91**, 254–258.

Rasmussen CE, Williams CKI (2006). *Gaussian Processes for Machine Learning. Adaptive Computation and Machine Learning*. MIT Press: Cambridge, MA.

Ren W, Lui S, Deng W, Li F, Li M, Huang X, Wang Y, Li T, Sweeney JA, Gong Q (2013). Anatomical and functional brain abnormalities in drug-naive first-episode schizophrenia. *American Journal of Psychiatry* **170**, 1308–1316.

Rocha-Rego V, Jogia J, Marquand AF, Mourao-Miranda J, Simmons A, Frangou S (2014). Examination of the predictive value of structural magnetic resonance scans in bipolar disorder: a pattern classification approach. *Psychological Medicine* **44**, 519–532.

Sarpal DK, Robinson DG, Lencz T, Argyelan M, Ikuta T, Karlsgodt K, Gallego JA, Kane JM, Szeszko PR, Malhotra AK (2015). Antipsychotic treatment and functional connectivity of the striatum in first-episode schizophrenia. *JAMA Psychiatry* **72**, 5–13.

Schrouff J, Rosa MJ, Rondina JM, Marquand AF, Chu C, Ashburner J, Phillips C, Richiardi J, Mourão-Miranda J (2013). PRoNTo: pattern recognition for neuroimaging toolbox. *Neuroinformatics* **11**, 319–337.

Smieskova R, Fusar-Poli P, Allen P, Bendfeldt K, Stieglitz RD, Drewe J, Radue EW, McGuire PK, Riecher-Rössler A, Borgwardt SJ (2009). The effects of antipsychotics on the brain: what have we learnt from structural imaging of schizophrenia? – a systematic review. *Current Pharmaceutical Design* **15**, 2535–2549.

Smith SM, Jenkinson M, Woolrich MW, Beckmann CF, Behrens TEJ, Johansen-Berg H, Bannister PR, De Luca M, Drobnjak I, Flitney DE, Niazy RK, Saunders J, Vickers J, Zhang Y, De Stefano N, Brady JM, Matthews PM (2004). Advances in functional and structural MR image analysis and implementation as FSL. *NeuroImage* **23** (Suppl. 1), S208–S219.

Song X-W, Dong Z-Y, Long X-Y, Li S-F, Zuo X-N, Zhu C-Z, He Y, Yan C-G, Zang Y-F (2011). REST: a toolkit for resting-state functional magnetic resonance imaging data processing. *PLoS ONE* **6**, e25031.

Spaniel F, Tintera J, Rydlo J, Ibrahim I, Kasparek T, Horacek J, Zaytseva Y, Matejka M, Fialova M, Slovakova A, Mikolas P, Melicher T, Görnerova N, Höschl C, Hajek T (2016). Altered neural correlate of the self-agency experience in first-episode schizophrenia-spectrum patients: an fMRI study. *Schizophrenia Bulletin* **42**, 916–925.

Sridharan D, Levitin DJ, Menon V (2008). A critical role for the right fronto-insular cortex in switching between central-executive and default-mode networks. *Proceedings of the National Academy of Sciences of the USA* **105**, 12569–12574.

Sundermann B, Herr D, Schwindt W, Pfleiderer B (2014). Multivariate classification of blood oxygen level-dependent fMRI data with diagnostic intention: a clinical perspective. *AJNR. American Journal of Neuroradiology* **35**, 848–855.

Swanson N, Eichele T, Pearlson G, Kiehl K, Yu Q, Calhoun VD (2011). Lateral differences in the default mode network in healthy controls and schizophrenia patients. *Human Brain Mapping* **32**, 654–664.

Takahashi T, Wood SJ, Yung AR, Phillips LJ, Soulsby B, McGorry PD, Tanino R, Zhou S-Y, Suzuki M, Velakoulis D, Pantelis C (2009). Insular cortex gray matter changes in individuals at ultra-high-risk of developing psychosis. *Schizophrenia Research* **111**, 94–102.

Takayanagi Y, Takahashi T, Orikabe L, Mozue Y, Kawasaki Y, Nakamura K, Sato Y, Itokawa M, Yamasue H, Kasai K, Kurachi M, Okazaki Y, Suzuki M (2011). Classification of first-episode schizophrenia patients and healthy subjects by automated MRI measures of regional brain volume and cortical thickness. *PLoS ONE* **6**, e21047.

Tzourio-Mazoyer N, Landeau B, Papathanassiou D, Crivello F, Etard O, Delcroix N, Mazoyer B, Joliot M (2002). Automated anatomical labeling of activations in SPM using a macroscopic anatomical parcellation of the MNI MRI single-subject brain. *NeuroImage* **15**, 273–289.

Venkataraman A, Whitford TJ, Westin C-F, Golland P, Kubicki M (2012). Whole brain resting state functional connectivity abnormalities in schizophrenia. *Schizophrenia Research* **139**, 7–12.

Vita A, De Peri L, Deste G, Sacchetti E (2012). Progressive loss of cortical gray matter in schizophrenia: a meta-analysis and meta-regression of longitudinal MRI studies. *Translational Psychiatry* **2**, e190.

Whelan R, Garavan H (2014). When optimism hurts: inflated predictions in psychiatric neuroimaging. *Biological Psychiatry* **75**, 746–748.

White TP, Joseph V, Francis ST, Liddle PF (2010). Aberrant salience network (bilateral insula and anterior cingulate cortex) connectivity during information processing in schizophrenia. *Schizophrenia Research* **123**, 105–115.

Zanetti MV, Schaufelberger MS, Doshi J, Ou Y, Ferreira LK, Menezes PR, Scazufca M, Davatzikos C, Busatto GF (2013). Neuroanatomical pattern classification in a population-based sample of first-episode schizophrenia. *Progress in Neuro-Psychopharmacology and Biological Psychiatry* **43**, 116–125.